Eur Biophys J (2004) 33: 732–741
DOI 10.1007/s00249-004-0420-5

ARTICLE

Jonas Henriksen · Amy C. Rowat · John H. Ipsen

Vesicle fluctuation analysis of the effects of sterols on membrane bending rigidity

Received: 6 January 2004 / Revised: 3 May 2004 / Accepted: 17 May 2004 / Published online: 25 June 2004

Abstract Sterols are regulators of both biological function and structure. The role of cholesterol in promoting the structural and mechanical stability of membranes is widely recognized. Knowledge of how the related sterols, lanosterol and ergosterol, affect membrane mechanical properties is sparse. This paper presents a comprehensive comparison of the effects of cholesterol, lanosterol, and ergosterol upon the bending elastic properties of 1-palmitoyl-2-oleoyl-*sn*-glycero-3-phosphocholine giant unilamellar vesicles. Measurements are made using vesicle fluctuation analysis, a nonintrusive technique that we have recently improved for determining membrane bending rigidity. Giving a detailed account of the vesicle fluctuation analysis technique, we describe how the gravitational stabilization of the vesicles enhances image contrast, vesicle yield, and the quality of data. Implications of gravity on vesicle behaviour are also discussed. These recent modifications render vesicle fluctuation analysis an efficient and accurate method for determining how cholesterol, lanosterol, and ergosterol increase membrane bending rigidity.

Keywords Lipid bilayer · Mechanical properties · Membrane elasticity

Abbreviations DMPC: Dimyristoylphosphocholine · POPC: 1-Palmitoyl-2-oleoyl-*sn*-glycero-3-phosphocholine · VFA: Vesicle fluctuation analysis · GUV: Giant unilamellar vesicle · TLC: Thin layer chromatography · EPR: Electron paramagnetic resonance · NMR: Nuclear magnetic resonance

J. Henriksen
MEMPHYS Centre for Biomembrane Physics,
Department of Chemistry, Technical University of Denmark,
2800 Lyngby, Denmark

A. C. Rowat
Department of Physics, University of Southern Denmark,
Campusvej 55, 5239 Odense, Denmark

J. H. Ipsen (✉)
Department of Chemistry, University of Southern Denmark,
Campusvej 55, 5239 Odense, Denmark
E-mail: ipsen@memphys.sdu.dk
Tel.: +45-6550-2560
Fax: +45-6615-8760

Introduction

Sterols are essential components of biological membranes and play an integral role in membrane organization, dynamics, and function, as well as in the structural integrity of the lipid bilayer. In eukaryotic cell membranes, cholesterol is the most abundant sterol, while the structurally similar ergosterol fills this role in fungi and protozoan membranes. The biosynthetic precursor of cholesterol and ergosterol, lanosterol, predominates in some prokaryotic membranes. Interactions of these sterols—in particular cholesterol—with membranes have been the subject of a vast number of experimental and theoretical biophysical investigations (Jacobs and Oldfield 1979; Ipsen et al. 1987; Vist and Davis 1990; Almeida et al. 1992; Urbina et al. 1995; Smondyrev and Berkowitz 2001; Endress et al. 2002a, 2002b; Miao 2002b).

Amongst these studies are a host of mechanical measurements of cholesterol–membrane systems. The stabilizing effect of cholesterol on membranes has been elucidated using various techniques such as micropipette aspiration, pressure extrusion, and vesicle fluctuation analysis. These studies reveal that cholesterol significantly increases the area expansion modulus, K_a (Needham et al. 1988; Endress et al. 2002a), the lysis tension, τ^* (Needham and Nunn 1990; Patty and Frisken 2003), and the bending rigidity modulus, κ (Duwe et al. 1990; Méléard et al. 1997). For example, κ of dimyristoylphosphocholine (DMPC) membranes was found to increase by ~80% upon the incorporation of 10 mol% cholesterol into the membrane (25 °C) (Méléard et al. 1997). A separate study found a ~250%

increase in κ of DMPC membranes with 30 mol% cholesterol (30 °C) (Duwe et al. 1990). The effects of lanosterol and ergosterol on membrane mechanical properties have been less extensively investigated. A recent micropipette aspiration investigation evaluated the effects of cholesterol, ergosterol, and lanosterol upon the area expansion modulus of DPPC membranes using 40 mol% sterol (Endress et al. 2002a). This study, together with other comparative biophysical investigations of these three sterols (Urbina et al. 1995; Endress et al. 2002a, 2002b), reveals that despite their structural similarities, the influence of these sterols upon membrane properties differs significantly.

To further explore how cholesterol, ergosterol, and lanosterol (Fig. 1) alter membrane elastic properties, we have investigated how these sterols affect the membrane bending rigidity, κ, of POPC giant unilamellar vesicles (GUVs) using vesicle fluctuation analysis (VFA). VFA is a noninvasive technique which can be used to infer membrane mechanical properties from the thermally induced shape fluctuations of fluid lipid membranes. As membranes are free-standing films with vanishing surface tension, their conformational stability is largely determined by the bending elasticity, κ. Other techniques which can be used to estimate κ on the level of a single vesicle include micropipette aspiration of vesicles in the low tension regime (Evans and Rawicz 1990) and deformation of a vesicle in an electric field (Niggeman et al. 1995). In contrast to VFA, both of these methods involve perturbing the membrane with an external force.

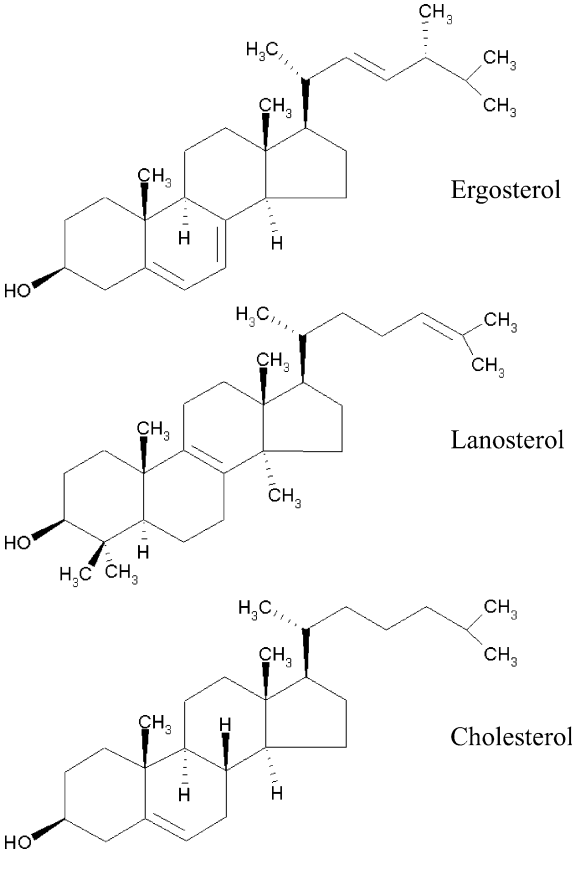

Fig. 1 Structures of ergosterol, lanosterol and cholesterol

Our understanding of the membrane flickering phenomenon as an interplay between thermally induced bending excitations and curvature elasticity dates back to Brochard and coworkers in the mid-1970s (Brochard and Lennon 1975; Brochard et al. 1976), who used this insight to estimate the bending rigidity of red blood cells. Despite some early applications of the technique to tubular and quasi-spherical vesicles (Schneider et al. 1984), the progress in its use has been slow. An effective method for preparing giant vesicles (Angelova and Dimitrov 1986; Angelova et al. 1992) as well as the necessary theoretical analysis (Faucon et al. 1989) and hardware for data collection and processing have furthered the development of the technique.

The spirit of the version of VFA presented in this paper follows the line of Faucon et al. (1989) where the Brownian excitations of quasi-spherical vesicle contours are analysed in detail. Our method, however, has been modulated in several respects to improve the efficiency: (1) use of real-time recording of vesicle contours; (2) use of a sucrose–glucose solution system (the GUVs contain sucrose and are resuspended in an equiosmolar glucose solution) which enhances image contrast and gravitationally stabilizes the vesicles due to the difference in molecular mass of the two sugars; and (3) reduction of the camera integration time for recording a vesicle contour snapshot. While gravitational stabilization offers some notable improvements (increased yield of vesicles near the bottom of the microscope observation chamber and stabilization of the vesicles during the acquisition of contour snapshots), gravity can also affect vesicle flicker behaviour; it is thus of major importance to control and understand the implications of this perturbation (Henriksen and Ipsen 2002). Together with an increased sample size, revisions in the data analysis procedure further improve the experimental error of VFA.

In this paper, we give a detailed account of the VFA procedure and describe our improvements upon the technique, focusing on experimental use and data analysis. These developments enhance both the experimental efficiency and accuracy as well as render the technique a more efficient method for analysing the elastic properties of biomembrane systems. Possible implications of gravity on the measurement of membrane bending elasticity, κ, are discussed. We describe the application of VFA in determining the effects of three structurally related sterols, cholesterol, lanosterol, and ergosterol, on the bending rigidity of POPC membranes.

Theory

The model

Fluid lipid membranes are soft and highly flexible objects which are susceptible to thermally induced shape

fluctuations. The length scales associated with the undulation phenomena of GUVs extend from the microscopic to the mesoscopic domain. Due to the optical length scale cutoff [1], only the longest wavelength shape deformations are observable by the use of light microscopy and can be analysed to obtain a measure of the membrane bending rigidity, κ.

As a consequence of this optical resolution, the total membrane area, A, is divided into a 'hidden' area stored on sub-optical length scales and an optically resolvable area, $\tilde{N}$. The 'hidden' area acts as an area reservoir which is in equilibrium with the observable area, $\tilde{N}$. The existence of such a reservoir is demonstrated in micropipette aspiration experiments where the undulations of apparently smooth vesicles are pulled out in the low tension regime (Evans and Rawicz 1990; Henriksen and Ipsen 2004). The model for the fluctuating vesicle can thus be defined in the grand canonical ensemble where the area in the optical regime is set by the tension, σ, which is conjugated to the total membrane area, A (Helfrich 1973).

Thermally induced membrane shape changes involve two types of elasticity. The first kind is related to out-of-plane bending which is primarily governed by the bending modulus, $\kappa \simeq 10$–$40\ \mathrm{k_B}T$. Area-stretching elasticity comprises the second class of elasticity and can be quantified by $K_a \simeq 0.1$–$1\ \mathrm{J/m^2} \simeq 10^7$–$10^8\ \mathrm{k_B}T/\mu\mathrm{m}^2$. As the energy change involved in area dilation is large compared to thermal energies ($\mathrm{k_B}T$), the membrane area is taken to be a constant. The internal volume of the vesicle is constrained due to osmotic balance (equiosmolar sugar solutions inside and outside the vesicle) (Seifert 1997; Henriksen and Ipsen 2002) and the membrane composition is constant due to the low solubility of PC lipids and these sterols in water.

At a continuum level, membrane shape changes can be described by the Helfrich Hamiltonian (Helfrich 1973),

$$\mathscr{H}_C = \sigma A + \frac{\kappa}{2}\int (2C - C_0)^2 \mathrm{d}A + \frac{\bar{\kappa}}{2}\int K \mathrm{d}A. \tag{1}$$

where the bending rigidity, κ, couples to the fluctuations in the mean curvature, $C = (1/R_1 + 1/R_2)/2$; and the Gauss modulus, $[(\bar{\kappa})]$, to the Gaussian curvature, $K = 1/(R_1\ R_2)^2$. Membrane asymmetry is described by the spontaneous curvature, C_0, which is essentially zero for a symmetric bilayer. The third term in Eq. (1) is a constant for fixed-vesicle topologies (Gauss-Bonnet theorem) and, as a consequence, is left out in the following where only quasi-spherical vesicles will be considered.

As the vesicle contains sucrose and is resuspended in a glucose solution, a transmembrane density difference, $\Delta\rho = \rho_{in} - \rho_{out}$, gives rise to an additional contribution:

$$\mathscr{H}_G = g\Delta\rho \int z \mathrm{d}V. \tag{2}$$

The integral in Eq. (2) is a summation of the vertical height, z, over the entire vesicle volume and g is the acceleration of gravity. The position of the quasi-spherical membrane surface,

$$\mathbf{x}(\theta,\phi) = R(1 + u(\theta,\phi))\mathbf{e}_R(\theta,\phi). \tag{3}$$

is given as a superposition of a perfect sphere with radius, R, and a local scalar perturbation field, $u(\theta,\phi)$, acting in the direction of the unit sphere normal, $\mathbf{e}_R(\theta,\phi)$, where θ and ϕ are the spherical angles. To describe fluctuations around the mean shape, the full Hamiltonian $\mathscr{H} = \mathscr{H}_C + \mathscr{H}_G$ is subsequently expanded to second order in $u(\theta,\phi)$ which in a spherical harmonic basis $\{Y_{lm}(\theta,\phi)\}$ condenses to[3]:

$$\mathscr{H} = 4\pi(2 + \Sigma) + \frac{1}{2}\sum_{lm} u_{lm}\mathbf{G}_{lm}^{-1}u_{lm} + \frac{g_0}{2}\sum_{lm}\sum_{l'm'} u_{lm}\mathbf{V}_{lml'm'}u_{l'm'} - \sum_{lm} h_{lm}u_{lm}. \tag{4}$$

Here, $\{u_{lm}\}$ is the spherical harmonic amplitudes, $G_{lm}^{-1} = \kappa(l-1)(l+2)|l(l+1) + \Sigma|$ is the stability matrix of the free-floating vesicle ($\Delta\rho = 0$); $\Sigma = \sigma \mathrm{R}^2/\kappa + {C_0}^2 R^2/2 + 2C_0 R$ is the effective reduced tension; $\mathbf{V}_{lml'\mathrm{m}'}$ is the perturbation matrix and $h_{lm} \neq 0$ only for $l = 1$ and 3, both terms which originate from the gravity contribution; and $g_0 = \Delta\rho \mathrm{gR}^4/\kappa$ (Henriksen and Ipsen 2002). At this point it is important to note that g_0 is a measure of the ratio of the gravitational and bending-energy scales, and therefore determines the size of the gravitational perturbation measured relative to the Hamiltonian for the free-floating vesicle. The parameter g_0 thus plays a key role in characterizing and quantifying the effect of gravity on the bending-energy measurement. Using perturbational theory and statistical mechanics, the free energy, mean amplitudes, $\langle u_{lm}\rangle$, and amplitude correlation functions, $\langle \delta \mathrm{u}_{lm} \delta \mathrm{u}_{l'\mathrm{m}'}{}^*\rangle$, can be calculated. The effect of gravity leads to new non-spherical mean shapes shown in Fig. 2 and a relative correction of the amplitude correlation function (Henriksen and Ipsen 2002):

$$\left\langle \delta u_{lm} \delta u_{l'm'}^* \right\rangle = \frac{G_{lm}\delta_{mm'}}{\beta}\left(\delta_{U'} + f(g_0, G_{lm}, V_{lml'm'})\right). \tag{5}$$

The effects related to the change in the mean shape and correlation function will be addressed in the following section where the coupling of the model and experimental observables is discussed.

Experimental observables

The vesicles undergo undulations in shape which can be observed using light microscopy and subsequently

[1] The optical resolution of a membrane displacement is of the order 100 nm at a 100-fold magnification level.

[2] R_1 and R_2 are the radii of curvature in the principal directions obtained from the Weingarten matrix.

[3] The notation Σ_{lm} will be used as an abbreviation of $\sum_{l=2}^{l_{cut}}\sum_{m=-l}^{l}$ where l_{cut} is the upper mode cutoff.

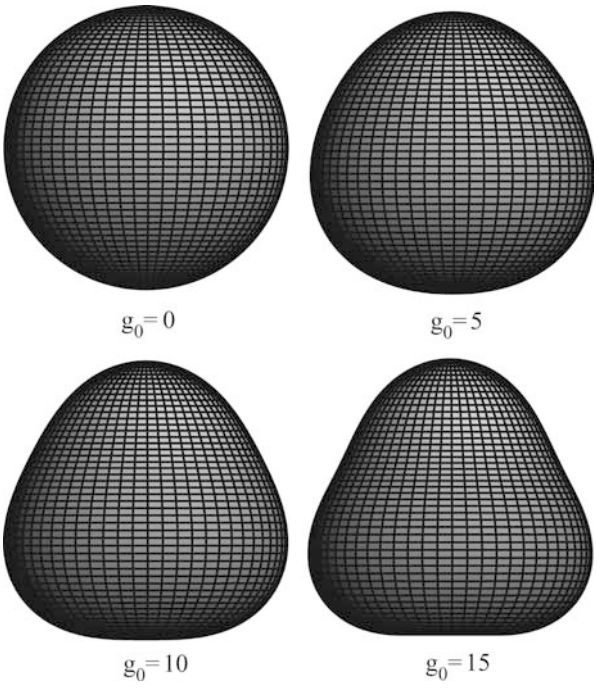

Fig. 2 Plot of the vesicle mean shape (*side view*) at four levels of g_0 and $\Sigma = 0$. The mean shape gradually changes from a sphere into a pear shape and the maximum cross section (*focal plane*) approaches the support (*bottom of the viewing chamber*) as a function of g_0. The mean shapes are given in increasing order of g_0 according to relationships published in Henriksen and Ipsen (2002)

analysed. This is accomplished by mounting a CCD-camera onto an inverted light microscope which is connected to a PC through a frame-grabber. The images from the frame-grabber are traced in real time and the data set containing the (x,y)-pixel contour coordinates is obtained. The trace of a membrane contour and the principle for obtaining the contour coordinates are illustrated in Fig. 3. The time required for the average interlaced CCD-camera to obtain (camera integration time, t_s) and process an interlaced image is $t_a \sim 40$ ms. Using non-interlaced mode (i.e. only every second line corresponding to one half-frame) to construct the contour data, the camera integration time can be lowered by one order of magnitude to $t_s = 2$–4 ms, but the spatial resolution is compromised. The reduced spatial resolution does not, however, come to affect the accuracy of the κ estimation. Note that while the reduced integration time allows for sampling over a much broader range of modes (see Data analysis below), the time between two consecutive images is still limited by the 25 frames/s capture rate (i.e. $t_a \sim 40$ ms between the acquisition of images). Approximately 3,000–4,000 contours must be captured to obtain good statistics for the ensemble average.

The information obtained in the microscope is only partial in the sense that it provides a two-dimensional view of the three-dimensionally fluctuating vesicle. To overcome this problem we follow the procedure developed by Faucon et. al. (1989) and introduce the angular correlation function,

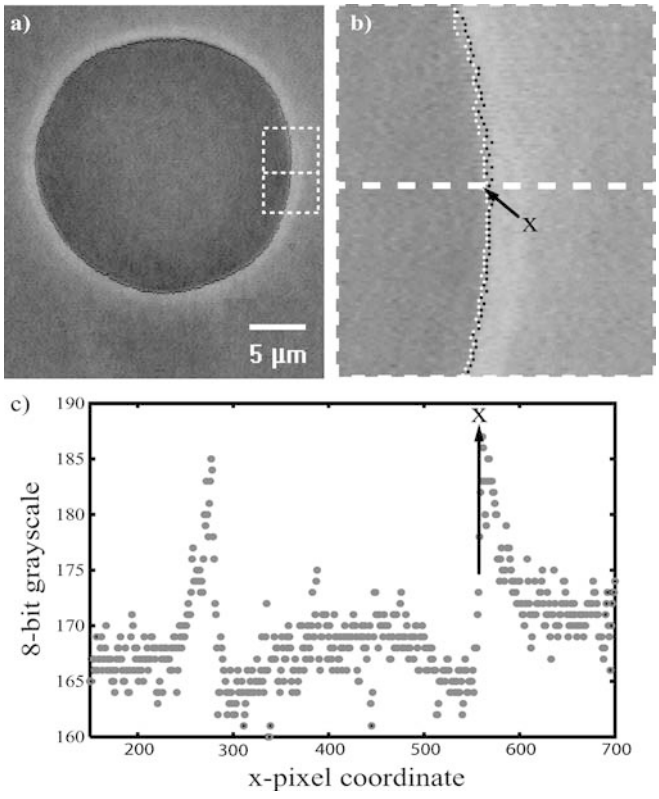

Fig. 3a–c The membrane position in the focal plane is analysed. **a** A 25-µm diameter vesicle and the corresponding trace of the membrane position are shown. **b** A magnification of the *dashed box* shown in **a**. The image from the frame-grabber is composed of two half-frames (the *black* and *white contour points*) obtained 20 ms apart. The relaxation times of the shortest membrane length scale fluctuations are smaller than 20 ms and the membrane thus moves during the capture of each half-frame. This effect is shown **b** where the half-frames have been traced separately, which gives rise to the contours shown in *black* and *white*. **c** The x,y-pixel coordinates of the membrane are defined by the largest gradient in the grey scale

$$\xi(\gamma,t) = \frac{1}{2\pi R^2}\int_0^{2\pi} \rho(\phi+\gamma,t)\rho^*(\phi,t)\mathrm{d}\phi - \frac{\bar{\rho}^2}{R^2}. \tag{6}$$

where $\rho(\phi,t)$ is the contour written in a polar representation at a given time t, and $\bar{\rho}$ is the ϕ-angle average of $\rho(\phi)$. In order to establish the connection to the amplitude correlation function, $\langle \delta u_{lm}\, \delta u^*_{l'm'} \rangle$, predicted by the model [Eq. (5)], Eq. (6) is expanded in a Legendre polynomial $\{P_l(\cos\gamma)\}$ basis:

$$B_l(t) = \left(\frac{2l+1}{2}\right)\int_{-1}^{1} P_l(\cos\gamma)\xi(\gamma,t)\mathrm{d}(\cos\gamma). \tag{7}$$

Here, $B_l(t)$ is a measure of the fluctuation amplitude of the lth spherical harmonic mode. The time average of $B_l(t)$ can be approximated as the ensemble average (see Data analysis below) which can in turn be fit to the model prediction based on Eq. (1) (explained in detail in Henriksen and Ipsen 2002):

$$\langle B_l(\kappa,\Sigma,g_0)\rangle = \langle B_l^0(\kappa,\Sigma)\rangle(1+b_l(g_0)). \tag{8}$$

Equation (8) is a product of the shape fluctuation amplitudes of a free-floating vesicle ($\Delta\rho = 0$) where

$$\left\langle B_l^0(\kappa, \Sigma) \right\rangle = \frac{2l+1}{4\pi\kappa\beta(l-1)(l+2)[l(l+1)+\Sigma]}. \qquad (9)$$

and $b_l(g_0)$, a relative correction term arising from gravity.

Correcting for gravity

The effect of gravity on the mean shape and shape fluctuation spectrum has been shown to be negligible for certain combinations of fitting ranges and values of g_0 and Σ (Henriksen and Ipsen 2002). In this section we will develop a tool for predicting when the effects of gravity on the estimate of κ are small.

In order to quantify the relative correction due to gravity for the shape fluctuation amplitudes, $\langle B_l(g_0)\rangle$, upper bounds, $|b_l(g_0)|$, for the relative correction are calculated numerically and plotted in Fig. 4. It can be observed (Fig. 4) that $|b_l(g_0)|$ decays rapidly with mode number, l, and saturates to a non-zero value reflecting the shift in the maximum cross section (Henriksen and Ipsen 2002). The relative correction is highly sensitive to the magnitude of the effective reduced tension, Σ (Fig. 4).

Based on the type of numerical data shown in Fig. 4, a domain in (Σ, g_0) is identified where $|b_l(g_0)| < b^{\text{crit}}$ for $l \geq l_{\min}$, b^{crit} being the chosen tolerance level below which the gravitational contribution is negligible. This is mapped out in Fig. 5 which can be used to quantify the maximal gravitational correction to the shape fluctuation spectrum based on estimates for the gravitational parameter g_0 and the effective tension Σ. Figure 5 thus provides a strong tool for deciding whether a particular measurement can be used as an estimate of κ or if it has to be rejected. For a typical vesicle of $R = 10$ μm and $\kappa = 40\ k_B T$ at 25 °C in a 75 mOsm sucrose–glucose solution ($\Delta\rho \sim 12$ kg/m^3), g_0 has a value of 7.4 (Fig. 5). For this particular example and a chosen acceptance criteria of $b^{\text{crit}} = 0.05$, a range for $l \geq 4$ can be analysed for $\Sigma \geq 5$, whereas the range $l \geq 3$ can be analysed for $\Sigma \geq 15$. Here, it is important to emphasize that an estimate for g_0 based on the sugar-solution densities is an upper bound since differences in phase contrast amongst vesicles in a population are observed.

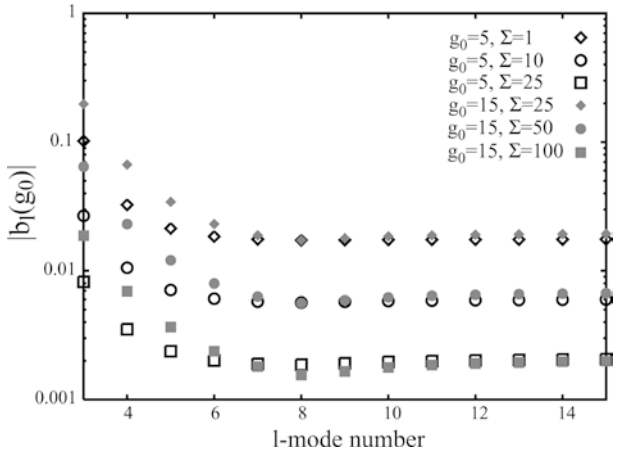

Fig. 4 Plot of the upper bounds for the relative correction to the shape fluctuation spectrum. Two levels of the gravitational parameter, g_0, are each shown for three values of the effective tension, Σ. It is observed that $|b_l(g_0)|$ decays as a function of l and saturates to a non-zero value for high l-modes. Moreover, the saturation value is strongly reduced for "tense" vesicles. As a consequence, the relative correction in the high l range can be reduced by increased levels of tension for large vesicles

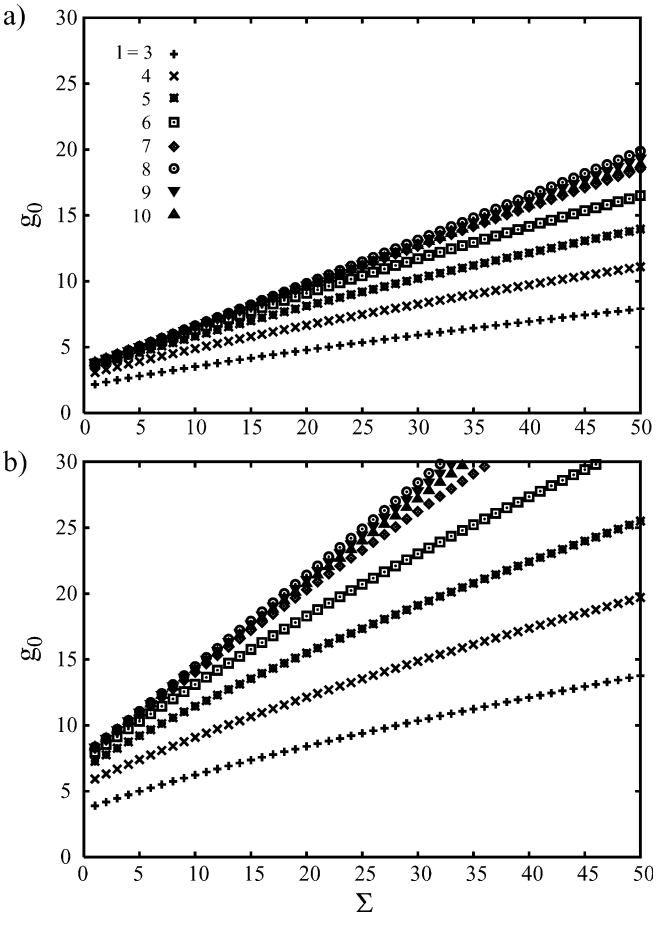

Fig. 5 Gravitational stability diagram plotted for individual l modes. The diagram can be used to determine whether the error on a measurement is tolerable given values of g_0 and Σ as well as $l_{\min}$ given a defined tolerance level, b^{crit}. Within the domain defined by the x-axis and the plotted lines, the relative correction from gravity, $|b_l(g_0)|$, is less than $b^{\text{crit}} = 1\%$ (**a**) and $b^{\text{crit}} = 5\%$ (**b**) for $l \geq l_{\min}$. For typical vesicles of $R = 5$–10 μm and $\kappa = 40\ k_B T$ at $T = 25$ °C in a 75 mOsm sugar solution ($\Delta\rho \sim 12$ kg/m^3), g_0 has a value of 0.5–40

Data analysis

In this section, procedures for analysing data will be discussed based on the theoretical prediction for the shape fluctuation spectrum. The main idea behind VFA

is to identify vesicles which have an acceptably small gravitational correction to their shape fluctuation spectra and thereafter resolve the bending rigidity and effective tension as fitting parameters by use of the expression developed for the free-floating vesicle [Eq. (9)].

In order to obtain the shape fluctuation spectrum, each contour is written in a polar representation[4]. The angular correlation function of the contour is subsequently calculated using Eq. (6) and the shape fluctuation amplitudes are obtained by Legendre polynomial transforms [Eq. (7)]. At this point the contour tracing is checked for outliers by inspection of the number of data points, N_c, constituting the contour. In Fig. 6a, the distribution of the number of points is plotted for a single vesicle experiment. The experimental shape fluctuation spectrum is obtained as an average over the time series $B_l(t)$:

$$\bar{B}_l(t_0) = \frac{1}{t_0}\int_0^{t_0} B_l(t)\mathrm{d}t. \tag{10}$$

where t_0 is the duration of the experiment. Due to the ergodic hypothesis, $B_l(t_0) \to \langle B_l \rangle$ for large t_0. To evaluate the quality of the estimate of $\langle B_l \rangle$, the variance of B_l is determined:

$$\sigma^2(\bar{B}_l(t_0)) = \frac{1}{t_0^2}\int_0^{t_0}\int_0^{t_0} C_{B_l}(t,t')\mathrm{d}t\mathrm{d}t'. \tag{11}$$

where $C_{B_l} = \langle \delta B_l(t)\delta B_l(t') \rangle$ is the autocorrelation function of B_l. For long time scales ($t-t' > \tau_l$), $C_{B_l}(t,t')$can be approximated by a single exponential decay in $|t-t'|$ with a characteristic relaxation time, τ_l (Milner and Safran 1987):

$$\tau_l = \frac{4\pi\eta R^3}{k_B T}\left(2 - \frac{1}{l(l+1)}\right)B_l \tag{12}$$

The viscosity of the sugar solution is approximated to be the same as water ($\eta \simeq 0.9\times10^{-3}$ kg m^{-1} s^{-1}) and $R \simeq 5$–15 μm is the radius of the vesicle. It should be noted that Eq. (12) is an approximation based solely on energy dissipation in the solvent and the elastic response of the membrane. A more sophisticated account of the relaxation dynamics has been reported (Miao et al 2002a). From Eq. (11), the variance of B_l is obtained:

$$\sigma\frac{2}{B_l} \simeq \begin{cases} \frac{2\tau_l}{t_0}\sigma^2_{B_l} & t_a < \tau_l << t_0 \\ \frac{t_a}{t_0}\sigma^2_{B_l} & t_s < \tau_l < t_a \end{cases}. \tag{13}$$

Here, $\sigma^2_{B_l} = (SDV)^2$ where SDV is the standard deviation of the amplitudes $B_l(t)$. In the time span $t \in [0;t_0]$, the number of uncorrelated time intervals is measured by $2\tau_l/t_0$ for $t_a < \tau_l < < t_0$. In the regime $t_s < \tau_l < t_a$, all the B_l modes ($\frac{t_0}{t_a}$) are uncorrelated in the time span $t \in [0;t_0]$. $B_l(t_0)$ has an approximately normal distribution with a variance given by Eq. (13). This allows for the definition of a distance between the experimentally obtained spectrum and the model prediction [Eq. (9)] by introducing the χ^2 function:

$$\chi^2 = \sum_{l=l_{\min}}^{l_{\max}} \left(\frac{\bar{B}_l(t_0) - \langle B_l^0(\kappa,\Sigma)\rangle}{\sigma_{B_l}}\right)^2. \tag{14}$$

The upper and lower bounds of the l-mode fitting range, $l_{\max}$ and $l_{\min}$, define the degrees of freedom for the χ^2 function by $f = l_{\max} - l_{\min} + 1$. The determination of these parameters will soon be discussed.

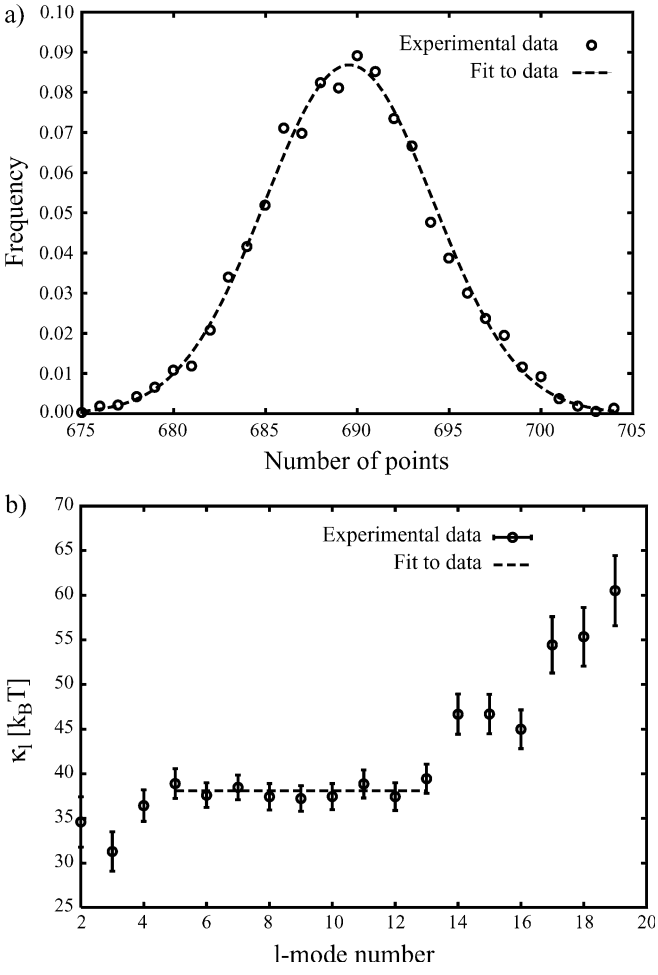

Fig. 6a, b Data representation of a single vesicle experiment, in this case, a POPC vesicle at $T = 25$ °C in 75 mOsm sucrose-glucose solution. **a** The frequency of the number of points constituting a contour. **b** The l mode-dependent bending rigidity as defined by Eq. (17). A plateau is identified in the range $l \in$ (Bivas et al. 1987; Endress et al. 2002b) where good agreement between the model and experiment are found. For $l > 5$ the gravitational correction is smaller than $b^{\mathrm{crit}} = 1\%$ which can be seen from Fig. 5a given $\Sigma = 25.5$ and $g_0 = 6.0$. The fit in the range $l \in$ (Bivas et al. 1987; Endress et al. 2002b) shown by the *dashed line* yields $\kappa = (38.1 \pm 0.9)$ $k_B T$ and $\Sigma = 25.5 \pm 2.2$. The quality of the fit is given by $P(\chi^2_m \leqslant \chi^2 | f) \simeq 12\%$ indicating a good fit

[4]The polar representation does not allow for overhangs, which results in the rejection of some contours. At this level it is necessary to make sure that all contours have the same direction of rotation in their polar representation.

The optimal fit is achieved when the χ^2 function is minimal which requires Eq. (14) to be stationary:

$$\left(\frac{\partial\chi^2}{\partial\kappa}\right)_{\Sigma}=0,\ \left(\frac{\partial\chi^2}{\partial\Sigma}\right)_{\kappa}=0. \tag{15}$$

In order to evaluate the goodness of a fit, the stochastic variable $\chi^2_m=\min\left(\chi^2\right)$ is considered. Given the correct model, the conditional probability $P\left(\chi^2_m\leqslant\chi^2|f\right)\in\chi^2(f)$ determines the likelihood that χ^2_m will be less than the observed value, χ^2. An acceptance criteria, $P\left(\chi^2_m\leqslant\chi^2|f\right)\leqslant 90\%$, is chosen. The variance of κ and Σ can be obtained from the covariance matrix (the inverse of the χ^2 stability matrix) evaluated at the minimum of χ^2:

$$\left[H_{ij}\right]=\begin{pmatrix}\frac{\partial^2\chi^2}{\partial\kappa^2} & \frac{\partial^2\chi^2}{\partial\kappa\partial\Sigma}\\ \frac{\partial^2\chi^2}{\partial\kappa\partial\Sigma} & \frac{\partial^2\chi^2}{\partial\Sigma^2}\end{pmatrix}^{-1}_{\min}. \tag{16}$$

The variances are obtained as $\sigma^2(\kappa)=H_{11}$ and $\sigma^2(\Sigma)=H_{22}$.

In Fig. 6b, data and the corresponding fit of a single vesicle experiment are presented. The plot shows the effective bending rigidity, κ_l, for the individual modes as a function of mode number, l:

$$\kappa_l^{-1}=4\pi\beta\bar{B}_l(t_0)\frac{(l-1)(l+2)[l(l+1)+\Sigma]}{2l+1}. \tag{17}$$

where $B(t_0)$ is the experimentally obtained spectrum and Σ a value obtained from the fit. In general, κ is estimated from the plateau region of the κ_l vs. l plot as shown in Fig. 6b. The lower bound of the fitting range, $l_{\min}$, should be chosen so that the gravitational correction of this mode does not exceed the defined criteria (Fig. 5). The upper bound is typically chosen to be $l_{\max}$ which fulfills $\tau_{l\max}\geq t_s$. The deviation of κ_l for $l>l_{\max}$ may be related to limited spatial and/or temporal resolution. The introduction of both these cut-off criteria as well as the estimate of $\sigma^2_{\bar{B}_l}$ makes our method different from that previously described by Faucon et al. (1989). In the following section, VFA will be used to investigate the mechanical stability of POPC membranes and a series of important sterols.

Materials and methods

POPC (1-palmitoyl-2-oleoyl-*sn*-glycero-3-phosphocholine) and cholesterol (98% pure) were obtained from Avanti Polar Lipids (Alabama, USA), ergosterol (≥97% pure) from Fluka (Buchs, Switzerland), and lanosterol (~97% pure) and solvents from Sigma-Aldrich (Denmark). Purity of the sterols was checked by thin-layer chromatography (TLC) using TLC aluminum sheets coated with silica gel (Merck, Darmstadt, Germany) in a hexane: ethyl acetate (1:1, v/v) solvent system. Upon spraying with 25% H_2SO_4 and subsequent incubation in a 90 °C oven, all sterols were found to be in one spot and thus pure. POPC and cholesterol were dissolved in methanol. Due to non-homogeneous mixing, methanol instead of chloroform was chosen for the lipid–cholesterol mixture (Vist and Davis 1990). Ergosterol and lanosterol were dissolved in 1:9 MeOH:$CHCl_3$ and 1:3 MeOH:$CHCl_3$. Solutions of ~0.1–0.3 mg of POPC/ml containing 10, 20 and 30 mol% sterols were prepared and 10 µl of the lipid/sterol mixture was deposited on platinum wire electrodes using a Hamilton syringe. The solvent was subsequently evaporated overnight in a vacuum chamber. GUVs were formed by electroformation (Angelova and Dimitrov 1986; Angelova et al. 1992) in a 75 mOsm sucrose solution at 25 °C, well above $T_m\simeq -5$ °C of the pure lipid. The vesicles were then resuspended in a 75 mOsm glucose solution contained in the thermostated observation chamber. Solution osmolarities were regulated using a freezing-point osmometer (Model 3D3, Advanced Instruments, Norwood, MA, USA) and MilliQ water was used throughout (Millipore, Bedford, MA, USA). Preparing the samples from a homogeneous mixture of lipids and sterols and considering the rapid transbilayer diffusion exhibited by cholesterol (Backer and Dawidowicz 1981) makes a homogeneous distribution of sterols in both monolayers a reasonable assumption.

Vesicle fluctuation analysis (VFA)

Vesicles were visualized at 25 °C using phase-contrast microscopy (Zeiss Axiovert S100, Göttingen, Germany). A CCD-camera (Sony, SSC-DP50AP) connected through a frame-grabber (Sigma-SLC, Matrix Vision, Oppenweiler, Germany) was used to capture a series of 3,000–4,000 vesicle contours in real time at a rate of 25 frames/s (non-interlaced). Shape fluctuation spectra were computed as described above. Each determined value for bending rigidity, κ, is an average of 10–20 different vesicles of diameter 15–30 µm.

Results

Figure 7 and Table 1 illustrate the effects of cholesterol, lanosterol, and ergosterol upon membrane bending rigidity, κ. Analysis of the data reveals increased levels of bending rigidity at 25 °C for POPC GUVs containing these sterols. The extent to which these compounds increase membrane order and thereby bending rigidity consistently follows the sequence cholesterol > lanosterol > ergosterol for the measured sterol concentrations. As observed in Fig. 7, κ increases monotonically as a function of sterol content for cholesterol and lanosterol whereas the effects of ergosterol saturate above ~20 mol%. The relative increases in κ at 10, 20 and 30 mol% sterol measured with respect to the bending rigidity of a pure POPC membrane at 25 °C are 41, 82 and 125% respectively for cholesterol; 34, 59 and 83%

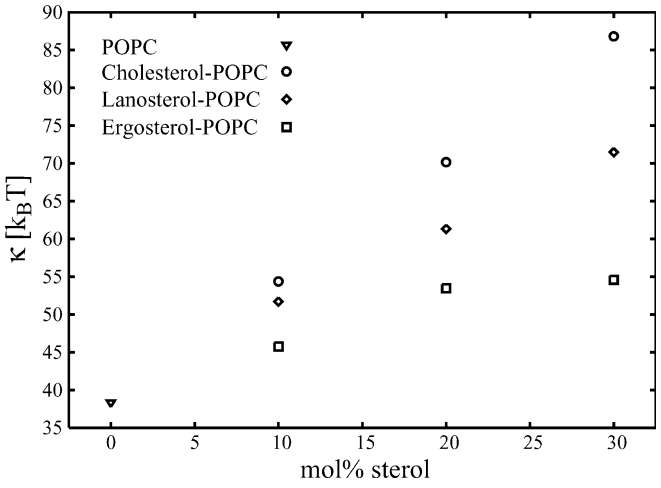

Fig. 7 Plot of bending rigidities as a function of the sterol content in POPC membranes (GUVs) at $T = 25$ °C. From the data it is observed that cholesterol has a larger effect than both lanosterol and ergosterol on membrane mechanical properties for all measured concentrations. Error is estimated to be less than ~3% and is reported in Table 1

Table 1 Bending rigidity,κ [k_BT], and mean standard error of POPC GUVs containing sterols at 25 °C

Sterol (mol%)	Cholesterol	Lanosterol	Ergosterol
0 (POPC)	38.5 ± 0.8		
10	54.4 ± 1.4	51.7 ± 1.2	45.8 ± 1.1
20	70.2 ± 0.8	61.3 ± 1.1	53.5 ± 1.7
30	86.8 ± 1.4	71.5 ± 0.6	54.6 ± 1.1

respectively for lanosterol; and 19, 39 and 42% respectively for ergosterol.

Discussion

Improvements on VFA

Gravitational stabilization of the vesicles greatly enhances the yield of vesicles in the focal plane. Not only does this modification make it possible to obtain a better time average of contours, it also makes it much more efficient to measure larger numbers of vesicles. The increased sample size greatly improves the statistics and thus decreases the experimental error for the determined κ value. As the membrane's spontaneous curvature, C_0, only shows up in the effective tension, Σ, it is therefore completely decoupled from the determination of κ; the small effects that low concentrations of sugars have upon C_0 (Döbereiner et al. 1999) thus do not perturb estimates of κ. Typically 10–20 GUVs out of a measured 40–60 vesicles qualify to constitute a data point after the elimination of contours with unacceptable gravitational corrections and/or defects (buds, interferences, incomplete contour traces, etc). Multilamellar vesicles can be detected both optically (observing the multilamellae and/or thicker outer rim) and/or by κ values that are significantly greater than the average κ value. The population of estimates for the bending rigidity is further analysed for outliers by use of statistical test theory (Student's t-test), which narrows the distribution and increases the reliability of the population mean value.

The effects of sterols on membrane bending rigidity

Upon incorporating cholesterol into POPC GUVs, κ increased markedly. The increase in κ was observed to be nearly proportional to the concentration of cholesterol (mol%) in the membrane.

Although performed with a different lipid membrane (DMPC, $T_m \simeq 24$ °C) at a different temperature (and thus different reduced temperature), the trend of our results is in agreement with previous measurements obtained by earlier versions of VFA. At 25 °C, 10 mol% cholesterol was observed to increase κ of DMPC vesicles by ~80% (Méléard et al. 1997). Well above the phase-transition temperature of the pure lipid at 40 °C, 10 mol% cholesterol increased κ by 45%, and 30 mol% by 142% with respect to pure DMPC membranes (Méléard et al. 1997). A separate study found 20 mol% cholesterol to increase κ of DMPC membranes by 83% and 30 mol% to induce a 248% increase at 30 °C (Duwe et al. 1990). How ergosterol and lanosterol affect membrane bending rigidity had not previously been investigated.

Sterols in context

Our VFA results on the membrane bending rigidity (κ) of POPC-sterol GUVs clearly show that cholesterol, lanosterol, and ergosterol all promoted membrane stability with cholesterol exerting the strongest effect: cholesterol > lanosterol > ergosterol. While this is the first comprehensive study of the membrane bending rigidity effects of these three sterols, other comparative biophysical studies have been undertaken. In these studies, sterol effects upon membrane physical properties were found to depend upon temperature and membrane composition.

Cholesterol, lanosterol and ergosterol were found to increase the area-expansion moduli of DPPC lipid membranes (Endress et al. 2002a) and increase the NMR order parameters of DMPC and POPC lipid membranes (Urbina et al 1995). The trend of the expansion moduli measurements published by Endress and co-workers (DPPC lipid membranes [$T_m \simeq 41$ °C] in the liquid ordered, l_o, phase) and the NMR measurements (DMPC lipid membranes well above the liquid ordered-disordered, l_o–l_d, coexistence region) published by Urbina et. al suggest the sequence ergosterol > cholesterol > lanosterol. These experiments reveal that ergosterol's ability

to order lipid membranes is strongly dependent upon the temperature relative to the main phase-transition temperature of the pure lipid, T_m. At temperatures well below T_m, ergosterol has the highest ordering ability: ergosterol > cholesterol > lanosterol. At temperatures well above T_m, the ordering sequence reverses to cholesterol > lanosterol > ergosterol, which correlates with our above-mentioned results.

Collectively this evidence suggests that the presence of a double bond and/or the temperature relative to T_m can influence sterol-lipid packing and thus membrane properties. The difference in effects upon membrane mechanical properties likely reflects differences in sterol-lipid packing. In contrast to cholesterol's flat sterol body, the trimethylated precursor lanosterol is furnished with bulky methyl groups while the sterol body of ergosterol is smooth like cholesterol.

The saturation effect of ergosterol above ~20 mol% observed in Fig. 7 has been previously observed (J. T. Thewalt, personal communication; Urbina et al 1995). Earlier electron paramagnetic resonance (EPR) of doxyl-fatty acid and cholestane spin-label probes in egg-PC membranes also revealed that ergosterol orders lipid chains up to 15–20 mol%. Above this concentration, ergosterol was found to induce disorder (Semer and Gerelinter 1979).

Conclusions

The VFA technique presented in this paper is well suited to investigating the notable effects sterols have upon membrane mechanical properties. Ultimately the technique provides a very effective way of measuring vesicle mechanical responses to modifications of membrane lipid composition. This allows for quantification of the effects related to changes in the lipid head group or fatty acid structure as well as determination of the influence of membrane stabilizing or destabilizing agents on membrane mechanical properties. Used to investigate the effects of cholesterol, lanosterol, and ergosterol upon POPC membranes, VFA reveals that all three molecules give rise to elevated bending rigidities to varying extents. Small differences in sterol structure can thus give rise to marked differences in membrane properties. Furthermore, it is clear that these effects are dependent upon the lipid composition (degree of unsaturation) and on reduced temperature. The ability of these sterols to modify membrane properties in different ways invites the question of the interplay amongst sterols, membrane mechanical properties, and evolution (Bloch 1976, 1983).

Acknowledgements Thanks to Martin J. Zuckermann, Jenifer L. Thewalt and Till Boecking for helpful sterol advice. MEMPHYS-Center for Biomembrane Physics is supported by the Danish National Research Foundation. A.C.R. is a Julie Payette Scholar sponsored by the Natural Sciences and Engineering Research Council (NSERC) of Canada.

References

Almeida PFF, Vaz WLC, Thompson TE (1992) Lateral diffusion in the liquid phases of dimyristoylphosphatidylcholine/cholesterol lipid bilayers. Biochemistry 31:6739–6747

Angelova MI, Dimitrov DS (1986) Liposome electroformation. Faraday Discuss Chem Soc 81:303–311

Angelova MI, Soléau S, Méléard PH, Faucon JF, Bothorel P (1992) Preparation of giant vesicles by external AC electric fields. Kinetics and applications. Prog Colloid Polym Sci 89:127–131

Backer JM, Dawidowicz EA (1981) Transmembrane movement of cholesterol in small unilamellar vesicles detected by cholesterol oxidase. J Biol Chem 256:586–588

Bivas I, Hanusse P, Bothorel P, Lalanne J, Aguerre-Chariol O (1987) An application of the optical microscopy to the determination of the curvature elastic modulus of biological and model membranes. J Physique 48:855–867

Bloch K (1976) On the evolution of a biosynthetic pathway. In: Kornberg A et al. (eds) Reflections on biochemistry. Pergamon Press, New York, p 143

Bloch KE (1983) Sterol structure and membrane function. CRC Crit Rev Biochem 19:47–92

Brochard F, Lennon JF (1975) Frequency spectrum of the flicker phenomenon in erythrocytes. J Physique 36:1035–1047

Brochard F, de Gennes PG, Pfeuty P (1976) Surface tension and deformations of membrane structures: relation to two-dimensional phase transitions. J Physique 37:1099–1104

Döbereiner HG, Selchow O, Lipowsky R (1999) Spontaneous curvature of fluid vesicles induced by trans-bilayer sugar asymmetry. Eur Biophys J 28:174–178

Duwe HP, Kaes J, Sackmann E (1990) Bending elastic moduli of lipid bilayers: modulation by solutes. J Phys Fr 51:945–962

Endress E, Bayerl S, Prechtel K, Maier C, Merkel R, Bayerl TM (2002a) The effect of cholesterol, lanosterol and ergosterol on lecithin bilayer mechanical properties at molecular and microscopic dimensions: a solid-state NMR and micropipet study. Langmuir 18:3293–3299

Endress E, Heller H, Casalta H, Brown MF, Bayerl TM (2002b) Anisotropic motion and molecular dynamics of cholesterol, lanosterol, and ergosterol in lecithin bilayers studied by quasi-elastic neutron scattering. Biochem 41:13078–13086

Evans E, Rawicz W (1990) Entropy-driven tension and bending elasticity in condensed-fluid membranes. Phys Rev Lett 64:2094–2097

Faucon JF, Mitov MD, Méléard P, Bivas I, Bothorel P (1989) Bending elasticity and thermal fluctuations of lipid membranes. Theoretical and experimental requirements. J Phys Fr 50:2389–2414

Helfrich W (1973) Elastic properties of lipid bilayers: theory and possible experiments. Z Naturforsch 28:693–703

Henriksen JR, Ipsen JH (2002) Thermal undulations of quasi-spherical vesicles stabilized by gravity. Eur Phys J 9:365–374

Henriksen JR, Ipsen JH (2004) Measurement of membrane elasticity by micro-pipette aspiration. Eur Phys J (in press)

Ipsen JH, Karlström G, Mouritsen OG, Wennerström H, Zuckermann MJ (1987) Phase equilibria in the phosphatidylcholine-cholesterol system. Biochim Biophys Acta 905:162–172

Ipsen JH, Mouritsen OG, Bloom M (1990) Relationships between lipid membrane area, hydrophobic thickness, and acyl-chain orientational order: the effects of cholesterol. Biophys J 57:405–412

Jacobs R, Oldfield E (1979) Deuterium nuclear magnetic resonance investigation of dimyristoyllecithin-dipalmitoyllecithin and dimyristoyllecitihin-cholesterol mixtures. Biochem 18:3280–3285

Méléard P, Gerbeaud C, Pott T, Fernandez-Puente L, Bivas I, Mitov MD, Dufourcq J, Bothorel J (1997) Bending elasticities of model membranes: influence of temperature and sterol content. Biophys J 72:2616–629

Miao L, Lomholt MA, Kleis J (2002a) Dynamics of shape fluctuations of quasi-spherical vesicles revisited. Eur Phys J E 9:143–160

Miao L, Nielsen M, Thewalt J, Ipsen JH, Bloom M, Zuckermann MJ, Mouritsen OG (2002b) From lanosterol to cholesterol: structural evolution and differential effects on lipid bilayers. Biophys J 82:1429–1444

Milner ST, Safran SA (1987) Dynamical fluctuations of droplet microemulsions and vesicles. Phys Rev A 36:4371–4379

Needham D, Nunn RS (1990) Elastic deformation and failure of lipid bilayer membranes containing cholesterol. Biophys J 58:997–1009

Needham D, McIntosh TJ, Evans E (1988) Thermomechanical and transition properties of dimyristoylphosphatidylcholine/cholesterol bilayers. Biochemistry 27:4668–4673

Nielsen M, Thewalt J, Miao L, Ipsen JH, Bloom M, Zuckermann MJ, Mouritsen OG (2000) Sterol evolution and the physics of membranes. Europhys Lett 52:368–374

Niggeman G, Kummrow M, Helfrich W (1995) The bending rigidity of phosphatidylcholine bilayers: dependences on experimental method, sample cell sealing and temperature. Phys II Fr 5:413–425

Patty PJ, Frisken BJ (2003) The pressure-dependence of the size of extruded vesicles. Biophys J 85:996–1004

Schneider MB, Jenkins JT, Webb WW (1984) Thermal fluctuations of large quasi-spherical bimolecular phospholipid vesicles. J Physique 45:1457–1472

Seifert U (1997) Configurations of fluid membranes and vesicles. Adv Phys 46:13–137

Semer R, Gerelinter E (1979) A spin label study of the effects of sterols on egg lecithin bilayers. Chem Phys Lipids 23:201–211

Smondyrev AM, Berkowitz ML (2001) Molecular dynamics simulation of the structure of dimyristoylphosphatidylcholine bilayers with cholesterol, ergosterol, and lanosterol. Biophys J 80:1649–1658

Urbina JA, Pekerar S, Le H, Patterson J, Montez B, Oldfield E (1995) Molecular order and dynamics of phosphatidylcholine bilayer membranes in the presence of cholesterol, ergosterol and lanosterol: a comparative study using ^{2}H-, ^{13}C- and ^{31}P-NMR spectroscopy. Biochim Biophys Acta 1238:163–167

Vist MR, Davis JH (1990) Phase-equilibria of cholesterol dipalmitoylphosphatidylcholine mixtures—H-2 nuclear magnetic resonance and differential scanning calorimetry. Biochem 29:451–264

Xu X, Bittman R, Duportail G, Heissler D, Vilcheze C, London E (2001) Effect of the structure of natural sterols and sphingolipids on the formation of ordered sphingolipid/sterol domains (rafts). J Biol Chem 276:33540–33546

Xu X, London E (2000) The effect of sterol structure on membrane lipid domains reveals how cholesterol can induce lipid domain formation. Biochemistry 39:843–849

Yeagle PL (1985) Lanosterol and cholesterol have different effects on phospholipid acyl chain ordering. Biochim Biophys Acta 815:33–36